Q3

Novel bis(thiosemicarbazones) of the 3,5-diacetyl-1,2,4-triazol series and their platinum(II) complexes: chemistry, antiproliferative activity and preliminary nephrotoxicity studies†

Ana I. Matesanz,[a] Carolina Hernández,[a,b] Ana Rodríguez[c] and Pilar Souza*[a]

Q1

The preparation and characterization of three novel [4]N-monosubstituted bis(thiosemicarbazone) ligands of 3,5-diacetyl-1,2,4-triazol series and their dinuclear platinum complexes are described. The crystal and molecular structure of the [Pt(μ-H₃L³)]₂ complex derived of 3,5-diacetyl-1,2,4-triazol bis([4]N-p-tolylthiosemicarbazone), H₅L³, has been resolved by single crystal X-ray diffraction. The ligands coordinate, in an asymmetric dideprotonate form, to the platinum ions in a tridentate fashion (NNS) and S-bridging bonding modes. Thus the molecular units of the platinum complexes are stacked as dimers. The new compounds synthesized have been evaluated for antiproliferative activity *in vitro* against NCI-H460, A2780 and A2780cisR human cancer cell lines. The cytotoxicity data suggest that these compounds may be endowed with important antitumour properties since are capable of not only circumventing cisplatin resistance in A2780cisR cells but also exhibit high antiproliferative activity in human non-small cell lung cancer NCI-H460 cells. The interactions of these compounds with calf thymus DNA was investigated by UV-vis absorption and a nephrotoxic study, in LLC-PK1 cells, has also been carried out.

Introduction

Although platinum metallo-drugs are among the most effective agents for the treatment of cancer its clinical utility is restricted due to the frequent development of drug resistance, the limited spectrum of tumours against which these drugs are active and severe normal tissue toxicity, including nephrotoxicity, being an important side effect which interferes with their therapeutic efficiency.[1–5]

These disadvantages have driven the development of improved platinum-based anticancer drugs but, the great majority of antitumour metal complexes synthesized are structural analogs of cisplatin and it has been demonstrated that these compounds having similar DNA-binding modes also exhibit similar biological profiles.

Therefore, there is a considerable interest in the synthesis and characterization of new structural types of compounds whose structure and mode of action differ from that of cisplatin.[6–9] In this regard, and taking into account that one of the mechanisms inducing the nephrotoxicity is due to the inactivation of some enzymes because of the reaction between platinum ions and sulfur containing proteins, an active area of research focuses on the synthesis of chelate platinum(II) complexes bearing nitrogen and sulfur mixed donor atoms, which should prevent the adverse reaction described.[10,11]

α-(N)-Heterocyclic thiosemicarbazones, (N)-TSCs, are typical tridentate NNS chelate ligands and moreover some of them have shown antineoplastic activity by themselves.[12] It has been demonstrated that the biochemical mechanism of action involves, among others, ribonucleotide reductase (RR) inhibition and DNA interaction by intercalation. Particularly, the 3-aminopyridine-2-carboxaldehyde thiosemicarbazone (Triapine, Vion Pharmaceuticals, New Haven, CT) is currently being screened for antitumour effects using the National Cancer Institute panel of 60 tumour cell lines and selected for Phase I and II clinical trials.[13–15]

For thiosemicarbazone/metal compounds, several mechanisms of antitumour action have also been proposed. For example, they a) could interact with DNA by formation of a metal-DNA covalent bond, b) could interfere in the DNA synthesis by RR inhibition, and c) could interact with DNA through non-covalent interactions including H-bonding and intercalation.[16]

Recently, investigations from our laboratory have led to the development of a series of 3,5-diacetyl-3,5-triazol bis([4]N-monosubstituted thiosemicarbazones).[17] The *in vitro* antitumour studies have shown that the 3,5-diacetyl-3,5-triazol

[a]*Departamento de Química Inorgánica (Módulo 07), Facultad de Ciencias, c/Francisco Tomás y Valiente n° 7, Universidad Autónoma de Madrid, 28049, Madrid, Spain. E-mail: pilar.souza@uam.es; Fax: (+34)914974833; Tel: (+34)914975156*

[b]*Departamento de Química Inorgánica, Orgánica y Bioquímica, Facultad de Ciencias del Medio Ambiente, Avd. Carlos III s/n, Universidad de Castilla-La Mancha, 45071, Toledo, Spain*

[c]*Departamento de Química Inorgánica, Orgánica y Bioquímica, ETS Ingenieros Industriales, Avd. Camilo José Cela n° 3, Universidad de Castilla-La Mancha, 13071, Ciudad Real, Spain*

bis(^4N-phenylthiosemicarbazone) ligand exhibits important antiproliferative activity in A2780 and A2780cisR human cancer cell lines. These observations prompted us to synthesize more analogous compounds by introducing a methyl substituent on the phenyl ring in *ortho*, *meta* and *para* positions to modify steric hindance and electronic effects of the ^4N-substituent. Thus, this work is aimed at describing the synthesis and chemical characterization of the new 3,5-diacetyl-1,2,4-triazol bis(^4N-tolylthiosemicarbazone) ligands, namely H_5L^1 (^4N-*ortho*-tolyl), H_5L^2 (^4N-*meta*-tolyl) and H_5L^3 (^4N-*para*-tolyl) and their dinuclear platinum(II) complexes [Pt(μ-H_3L^1)]$_2$, [Pt(μ-H_3L^2)]$_2$ and [Pt(μ-H_3L^3)]$_2$, respectively (Scheme 1).

In order to investigate the influence of ^4N-substitution on the antitumour activity, the new compounds synthesized have been evaluated for antiproliferative activity *in vitro* against three human cancer cell lines: NCI-H460 (non-small cell lung cancer), A2780 and A2780cisR (epithelian ovarian cancer). The interaction of these compounds with calf thymus DNA (CT-DNA) was also investigated. In addition nephrotoxicity studies, on normal human renal LLC-PK1 cells, have been carried out as an attempt to provide an insight into the pharmacological properties of these compounds.

Results and discussion
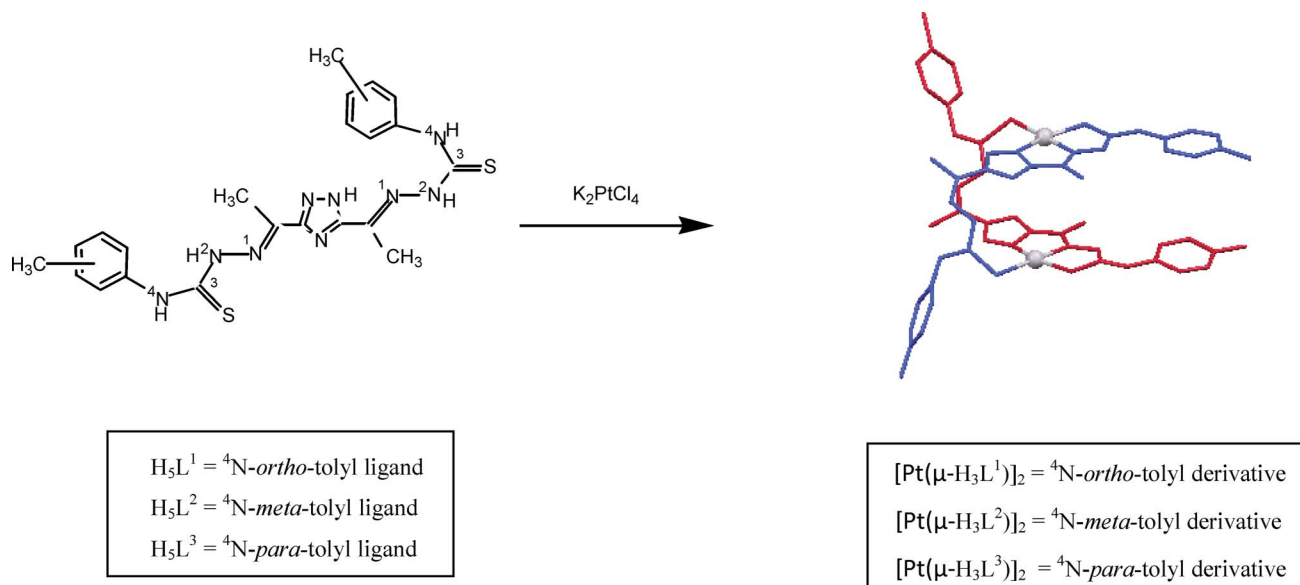
Synthesis and spectroscopic characterization

Three new ^4N-monosubstituted bis(thiosemicarbazone) ligands have been synthesized with high purities and acceptable yields. The compounds, obtained as ethanol solvates, are yellow powders, stable to air and moisture and were characterized by elemental analysis, FAB$^+$ spectrometry and IR and ^1H NMR spectroscopy.

3,5-diacetyl-1,2,4-triazol bis(^4N-tolylthiosemicarbazone) ligands react with K_2PtCl_4 to yield, stable to air and moisture, orange platinum(II) complexes [Pt(μ-H_3L^1)]$_2$, [Pt(μ-H_3L^2)]$_2$ and

[Pt(μ-H_3L^3)]$_2$. Analytical and spectroscopic results are consistent with the formation of the neutral non-conducting species.

The significant IR vibrational bands and the ^1H chemical shift values of the free ligands and their platinum(II) complexes are listed in the experimental section and Scheme 1 shows the numbered structure of the free ligands. Comparison of the IR spectra of the complexes with that of the free ligands show the expected differences given the dideprotonation and coordination shown by the X-ray study of [Pt(μ-H_3L^3)]$_2$, thus, the ν(NH-triazol) disappears in the spectra of platinum complexes as consequence of the deprotonation of the triazole ring. Regarding the typical bands from the thioamide group,[18] –NH–C(S)–, which are expected to be affected differently by different modes of coordination after complexation with metal ions, the band corresponding to ν(C=S) disappears upon complexation indicating coordination *via* the thioamide sulfur atom. On the other hand, coordination only induces minor changes in ν(C=N).

In the ^1H NMR spectra of the ligands, the triazolic proton was observed as a singlet between 15.09 and 15.28 ppm and two independent singlets at ~12.9 and ~11.3 ppm were observed for ^2N-hydrazinic hydrogens suggesting the presence of the *Z* (sulfur atom *cis* to the azomethine nitrogen atom) and *E* (sulfur atom *trans* to the azomethine nitrogen atom) structural isomers in solution in accordance with data reported in the literature for other thiosemicarbazones.[19] It may be surprising that these three signals remain in the spectra of the dimeric dideprotonated complexes, however this fact can be explained taking in account that the complexes are dimeric and contain four thiosemicarbazone arms which can exist, in solution, in various tautomeric forms (asymmetric dideprotonation, or symmetric deprotonation) forming both intra- and intermolecular hydrogen bonds. The ^1H NMR integration values of these signals in the complexes (0.5 : 0.5 : 1) are in agreement with the loss of two protons upon complexation. The rest of the proton signals appear, in the complexes, at nearly identical positions if each one is compared with its corresponding parent ligand.

$H_5L^1 = {}^4N$-*ortho*-tolyl ligand
$H_5L^2 = {}^4N$-*meta*-tolyl ligand
$H_5L^3 = {}^4N$-*para*-tolyl ligand

[Pt(μ-H_3L^1)]$_2 = {}^4N$-*ortho*-tolyl derivative
[Pt(μ-H_3L^2)]$_2 = {}^4N$-*meta*-tolyl derivative
[Pt(μ-H_3L^3)]$_2 = {}^4N$-*para*-tolyl derivative

Scheme 1   Structure of bis(thiosemicarbazone) ligands and their dinuclear platinum complexes.

Table 1 Crystal data and structure refinement for **[Pt(µ-H₃L³)]₂** compound

Molecular formula	$C_{44}H_{46}N_{18}Pt_2S_4$
Formula weight	1345.43
T/K	230(2)
Wavelength (Å)	0.71073
Crystal system	Triclinic
Space group	$P\bar{1}$
a/Å	14.654(4)
b/Å	16.423(8)
c/Å	17.538(8)
α (°)	117.584(11)
β (°)	97.032(17)
γ (°)	105.311(18)
Volume/Å³	3457(2)
Z	2
Density (calculated) (g cm⁻³)	1.292
Absorption coefficient (mm⁻¹)	4.201
$F(000)$	1312
Crystal size/mm	$0.20 \times 0.06 \times 0.05$
Index ranges	$-18 \leq h \leq 17, -16 \leq k \leq 20, -21 \leq l \leq 10$
Reflections collected	21429
Independent reflections	13682 [R(int) = 0.0391]
Data/restraints/parameters	13682/432/621
Goodness-of-fit on F^2	0.968
Final R indices [$I > 2\sigma(I)$]	$R_1 = 0.0518$, w$R_2 = 0.1398$
R indices (all data)	$R_1 = 0.0775$, w$R_2 = 0.1508$
Largest diff. peak and hole, e Å⁻³	0.924 and −0.677

Table 2 Selected bond distances (Å) and angles (°) for **[Pt(µ-H₃L³)]₂** complex

S(1)–C(1)	1.792(10)	S(1)–Pt(1)–S(4)	95.60(9)
S(2)–C(15)	1.733(8)	S(1)–Pt(1)–N(1)	84.2(2)
S(3)–C(23)	1.807(10)	S(1)–Pt(1)–N(4)	164.0(2)
S(4)–C(37)	1.745(9)	S(4)–Pt(1)–N(1)	179.6(2)
C(1)–N(2)	1.315(11)	S(4)–Pt(1)–N(4)	100.4(2)
C(1)–N(3)	1.385(10)	N(1)–Pt(1)–N(4)	79.9(3)
C(23)–N(3)	1.433(11)	S(2)–Pt(2)–S(3)	96.30(9)
C(23)–N(11)	1.32(1)	S(3)–Pt(2)–N(10)	85.1(2)
C(15)–N(2)	1.387(8)	S(3)–Pt(2)–N(13)	164.6(2)
N(10)–N(11)	1.431(9)	S(2)–Pt(2)–N(10)	179.9(2)
Pt(1)–S(1)	2.282(3)	S(2)–Pt(2)–N(13)	99.0(2)
Pt(1)–S(4)	2.327(2)	N(10)–Pt(2)–N(13)	79.6(3)
Pt(2)–S(2)	2.323(2)		
Pt(2)–S(3)	2.298(2)		
Pt(1)–N(1)	2.034(7)		
Pt(1)–N(4)	2.046(7)		
Pt(2)–N(10)	2.023(7)		
Pt(2)–N(13)	2.054(7)		

These spectroscopic similarities suggest the same dimeric structure for the three platinum(II) complexes synthesized.

Description of the crystal structure

Good quality crystals suitable for single crystal X-ray diffraction analysis were obtained for [Pt(µ-H₃L³)]₂ by recrystallization in dimethylsulfoxide (DMSO). The molecular structure of the platinum complex together with the atomic numbering scheme is shown in Fig. 1. Crystallographic data is shown in Table 1 with selected bond lengths shown in Table 2.

This neutral platinum(II) dinuclear compound crystallizes in the triclinic $P\bar{1}$ space group with $Z = 2$ and its crystallographic analysis reveals unambiguously a dimeric structure which results
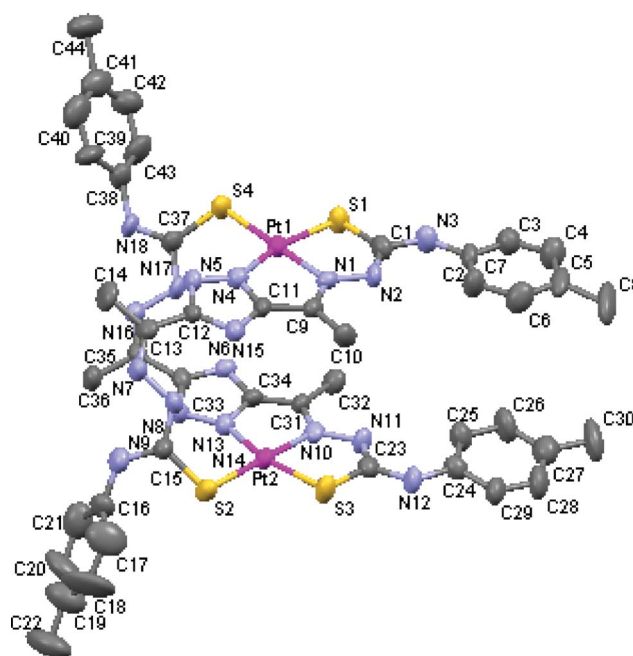
Fig. 1 Molecular structure of **[Pt(µ-H₃L³)]₂** (hydrogen atoms are omitted for clarity).

from the pairing of two mononuclear subunits through two thiosemicarbazone moieties bridges.

Each Pt(II) center is four coordinated with a [NNSS] donor environment, via: one triazolic nitrogen atom, the iminic nitrogen and sulfur atoms belonging to the deprotonated arm of one ligand molecule, and the fourth position being occupied by a sulfur atom of the non-deprotonated arm from the other ligand. Thus, the deprotonated thiosemicarbazone arm behaves as a bidentate and the neutral one behaves as a monodentate acting as a bridge.

The bond angle data indicates that the stereochemistry around each platinum(II) ion is almost planar. The angles deviate slightly from that expected for a regular square-planar geometry, this distortion may be attributed to the restricted bite angle of the tridentate moieties. The coordination results in the formation of two five membered (PtSCNN and PtSCNN) chelate rings for each platinum(II) ion, which are coplanar with the deprotonated triazole ring.

The Pt–N [2.024–2.054 Å] and Pt–S [2.282–2.327 Å] bond distances are comparable with those reported for Pt(II) thiosemicarbazone complexes.[20–22] It is important to note that upon coordination, the deprotonated arms undergo significant evolution from the thione to the thiol form [C(1)–S(1) 1.792(10) and C(23)–S(3) 1.807(10) Å], while the neutral thiosemicarbazone arms present shorter C–S bond lengths [C(37)–S(4) 1.755(9) and C(15)–S(2) 1.733(8) Å]. The C–N and N–N bond distances are intermediate between formal single and double bonds, pointing to extensive delocalization over the entire 3,5-diacetyl-1,2,4-triazole bis(thiosemicarbazone) skeleton.

Interestingly, the flexibility of the ligand originating from the free rotation of the two thiosemicarbazone arms around the C(9)–C(11), C(12)–C(13), and C(31)–C(34), C(33)–C(35) single bonds, allows each ligand to ligate to two metal ions in a twist conformation generating two parallel coordination planes.[23] Particularly, between the two triazole moieties, the interplane

Table 3 *In vitro* antiproliferative activity of the bis(thiosemicarbazone) compounds and cisplatin, evaluated in human *NCI-H460* (*non-small lung cancer*), *A2780* and *A2780cisR* (*epithelian ovarian cancer*) cell lines

	A2780		A2780cisR			NCI-H460	
	%Inhibition(100 μM)	IC$_{50}$(μM)	%Inhibition(100 μM)	IC$_{50}$(μM)	RF^a	%Inhibition(100 μM)	IC$_{50}$(μM)
H$_5$L^1·EtOH	91 ± 1	8.2 ± 0.19	93 ± 1	15 ± 1	(1.8)	65 ± 1	17 ± 1
H$_5$L^2·EtOH	94 ± 1	3.0 ± 0.02	92 ± 1	5.0 ± 0.05	(1.7)	87 ± 2	7.4 ± 0.41
H$_5$L^3·EtOH	90 ± 2	3.7 ± 0.02	93 ± 1	3.8 ± 0.4	(1.0)	85 ± 1	13 ± 2
[Pt(μ-H$_3$L^1)]$_2$	86 ± 1	7.4 ± 0.08	91 ± 1	15 ± 1	(2.0)	60 ± 2	17 ± 1
[Pt(μ-H$_3$L^2)]$_2$	93 ± 1	16 ± 1	90 ± 1	35 ± 1	(2.2)	45 ± 4	> 100
[Pt(μ-H$_3$L^3)]$_2$·2DMSO	88 ± 1	2.6 ± 0.04	92 ± 1	4.9 ± 0.06	(1.9)	60 ± 2	6.3 ± 0.26
Cisplatin	94 ± 1	0.85 ± 0.02	90 ± 3	5 ± 0.5	(5.9)	90 ± 2	5.9 ± 0.2

^{a} RF, resistance factor (n-fold) in parentheses. The fold resistance equals the IC$_{50}$ of the resistant cell divided by the IC$_{50}$ of the parental cells.

separation being 3.43 Å is considered optimal for π–π interactions (intramolecular stacking). This arrangement is reinforced by double intramolecular hydrogen bonds between the ^{2}NH of the bridging thiosemicarbazone moieties and uncoordinated triazole nitrogen atoms. The crystal lattice is further stabilized by intermolecular π–π stacking interactions between successive thiosemicarbazone moieties (3.78 Å) that give rise to the environment for the structure that is represented in Fig. 2.

Antiproliferative activity in human NCI-H460, A2780 and A2780cisR cell lines

To analyze the potential of the compounds as antitumour agents, the new compounds synthesized were tested (in powder solid form) for their antiproliferative activity *in vitro* against the human cancer cell lines: NCI-H460 (non-small cell lung cancer),

A2780 and A2780cisR (ephileian ovarian cancer). For comparison purposes the cytotoxicity of cisplatin was evaluated under the same experimental conditions.

Table 3 shows that the three new ligands present important antiproliferative activity in both A2780, cisplatin sensitive, and A2780cisR, cisplatin resistant cell lines. Of particular relevance are the values of the resistance factor, RF (defined as IC$_{50}$ in A2780cisR/IC$_{50}$ in A2780) which indicate that the three ligands are able to circumvent cisplatin resistance. The ligands also exhibit antiproliferative activity in NCI-H460 cell line having IC$_{50}$ values in the low micromolar range.

From the chemical point of view, the position of the methyl group on the tolyl ring does not appear to influence cytotoxicity since the antiproliferative activity of the ligands [H$_5$L^1 (^{4}N-*ortho*-tolyl), H$_5$L^2 (^{4}N-*meta*-tolyl) and H$_5$L^3 (^{4}N-*para*-tolyl)] is comparable in the three lines tested.
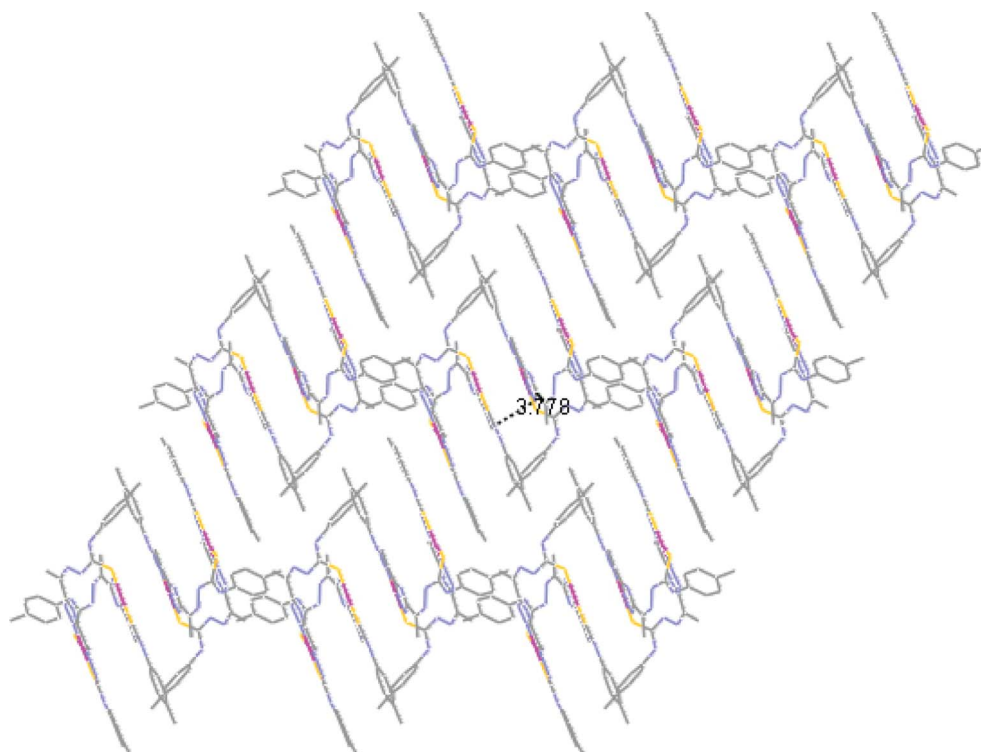

Fig. 2 View of **[Pt(μ-H$_3$L^3)]$_2$**, along the *bc* plane, showing the parallel disposition of the molecules as a result of π–π stacking interactions.

Upon complexation, the three resulting complexes [Pt(μ-H₃L¹)]₂, [Pt(μ-H₃L²)]₂ and [Pt(μ-H₃L³)]₂ also show antiproliferative activity, in both A2780 and A2780cisR, in the low micromolar range. The RF values of 2.0, 2.2 and 1.9, lower than that of cisplatin (5.9), indicate that the three complexes are able to circumvent cisplatin resistance. In contrast, NCI-H460 cell line show distinctive sensitivity to the platinum complexes, thus [Pt(μ-H₃L¹)]₂ and [Pt(μ-H₃L³)]₂, with the methyl group in the *ortho* and *para* positions of the phenyl ring respectively, were comparable in activity to cisplatin while the *meta*-tolyl substituted, complex [Pt(μ-H₃L²)]₂, show minimal activity (inhibition of 45% at the maximum concentration of 100 μM).

DNA Binding Studies

To study the binding affinity between DNA and the new ligands and platinum(II) complexes, which have significant effect against the tested cell lines, the UV absorption spectroscopy has been a very useful technique because the typical B-form DNA gives rise to a characteristic band at 260 nm in UV region. Hyperchromism (increase in absorption of the DNA band) and hypochromism (decrease in absorption of the DNA band) are the spectral changes typical of a compound interaction with the DNA helix. Hypochromism results from contraction of the DNA helix as well as changes in its conformation, while hyperchromism results from damage to the DNA double helix structure.[24]

In UV experiments, the spectra of CT-DNA in the presence of each compound have been recorded, by keeping constant CT-DNA concentrations in diverse [CT-DNA]/[compound] mixing ratios ($R = 1$–10) and monitoring the change in the absorption intensity of the typical CT-DNA spectral band at 260 nm.

In the absence of CT-DNA, both ligands and complexes displayed intense absorptions bands in the UV region (λ_{max} 295–323 nm) assigned to intraligand $\pi \rightarrow \pi^*$ transitions of aromatic chromophores which are also sensitive to the interaction of the compound with CT-DNA.

For all compounds, the absorption spectra displayed an increase in the intensity of the characteristic CT-DNA absorbance while increasing the compound concentration, and the percentage of hyperchromism observed is given in Table 4. Only in the spectrum of H₅L¹ ligand, the hyperchromism is accompanied by a red-shift up to 275 nm. In addition, the absorption spectra of the three ligands show an increase of the intensity of the ligand centered transitions, and these changes are also more pronounced in the case of H₅L¹ ligand for which the band at λ_{max} 322 nm is split into three bands at λ_{max} 327, 241 and 357 nm (Fig. 3).

Table 4 Absorption spectral properties of bis(thiosemicarbazone) ligands and their platinum(II) complexes bound to CT-DNA

	Increase in absorbance (%)[a]
H₅L¹·EtOH	65
H₅L²·EtOH	55
H₅L³·EtOH	60
[Pt(μ-H₃L¹)]₂	50
[Pt(μ-H₃L²)]₂	70
[Pt(μ-H₃L³)]₂·2DMSO	60

[a] % hyperchromism = $(A_{DNA\ bound} - A_{DNA\ free})/A_{DNA\ bound}$

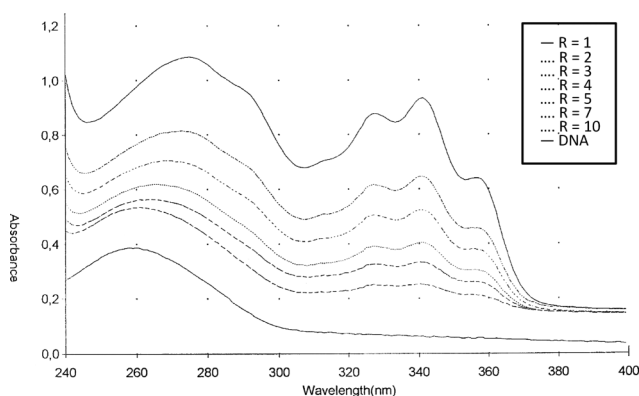**Fig. 3** UV absorption spectra of CT-DNA in absence (bottom) and presence of H₅L¹·EtOH ligand. The data were collected for [CT-DNA] = 1×10^{-4} M and mixing ratio R of 1, 2, 3, 4, 5, 7 and 10 (from top to bottom).

These characteristics suggest noncovalent interactions such as electrostatic and surface (major or minor groove) binding along the outside of the DNA helix. Intercalative DNA-binding has been excluded on the basis of the absence of hypochromism; in the other hand both ligands and platinum(II) complexes show similar UV absorption profiles therefore a covalent interaction between Pt(II) and guanine N7 is unlikely.

Preliminary nephrotoxicity studies

In order to investigate possible adverse side effects that may occur, such as nephrotoxicity, the compounds were subsequently tested (in powder solid form) *in vitro* on normal human renal LLC-PK1 cells. For comparison purposes the toxicity of cisplatin was evaluated under the same experimental conditions.

As is shown in Table 5, the [Pt(μ-H₃L¹)]₂ complex exhibited very low cellular growth inhibition (<50%), at the maximum concentration of 100 μM, and therefore did not have evaluable cytotoxicity (IC₅₀ > 100 μM). In addition, compounds H₅L¹ and [Pt(μ-H₃L²)]₂ were demonstrated to be much less toxic (over 5 fold) to the LLC-PK1 cells than cisplatin by comparing their IC₅₀.

The three remaining compounds H₅L², H₅L³ and [Pt(μ-H₃L³)]₂ have nephrotoxic profiles similar to that of cisplatin but also similar cytotoxic profiles with the advantage of circumventing cisplatin resistance in the A2780cisR cell line.

Table 5 *In vitro* antiproliferative activity of the bis(thiosemicarbazone) compounds and cisplatin, evaluated in normal human LLC-PK1 renal cells

	LLC-PK1	
	%Inhibition (100 μM)	IC₅₀ (μM)
H₅L¹·EtOH	54 ± 1	43 ± 4
H₅L²·EtOH	80 ± 3	9.5 ± 0.62
H₅L³·EtOH	79 ± 2	14 ± 2
[Pt(μ-H₃L¹)]₂	47 ± 2	> 100
[Pt(μ-H₃L²)]₂	55 ± 2	44 ± 3
[Pt(μ-H₃L³)]₂·2DMSO	62 ± 2	8.7 ± 0.14
Cisplatin	85 ± 1	7.9 ± 0.09

Conclusion

The compounds investigated here are capable not only of circumventing cisplatin resistance in A2780cisR cells but also exhibit high antiproliferative activity in human non-small cell lung cancer NCI-H460 cells with the only exception of [Pt(μ-H$_3$L^2)]$_2$. Taking into account that these compounds are active in A2780cisR cisplatin resistant cells and moreover, both ligands and platinum(II) complexes do efficiently interact with CT-DNA by inducing structural changes on the DNA secondary structure different from those induced by cisplatin, it is most likely that part of the biochemical mechanism of action of these bis(thiosemicarbazone) compounds involves groove binding. The compounds synthesized here are neutral, aromatic and hydrophobic molecules and therefore should tend to accumulate within the lypophilic DNA grooves.

In conclusion, this study indicates that the newly synthesized bis(thiosemicarbazone) ligands and platinum(II) complexes may be endowed with important antitumour properties. Moreover these compounds show less nephrotoxity than cisplatin on LLC-PK1 cells, and the platinum complex [Pt(μ-H$_3$L^1)]$_2$ being the most promising compound of this new series since it is active in the low micromolar range but not nephrotoxic at 100 μM. Based on these results, these compounds represent a valuable lead in the development of new anticancer chemotherapeutic agents capable of improving antitumour activity and reducing nephrotoxicity.

Experimental

Measurements

Elemental analyses were performed on a LECO CHNS-932 microanalyzer. Fast atom bombardment (FAB) mass spectra were performed on a VG AutoSpec spectrometer (nitrobenzyl alcohol matrix). ^{1}H NMR spectra (DMSO-d_6) were recorded on a BRUKER AMX-300 spectrometer. All cited physical measurements were obtained out by the Servicio Interdepartamental de Investigación (SIDI) of the Universidad Autónoma de Madrid.

Melting points were determined with a Stuart Scientific SMP3 apparatus. Conductivity measurements were made on a Crison Basic 30+ conductimeter. Infrared spectra (KBr pellets) were recorded on a Bomen–Michelson spectrophotometer (4000–400 cm^{-1}). Electronic spectra were recorded on an Unicam UV/vis UV4 spectrophotometer.

Materials

Solvents were purified and dried according to standard procedures. Hydrazine hydrate, L-lactic acid, *ortho*-tolyl isothiocyanate, *meta*-tolyl isothiocyanate, *para*-tolyl isothiocyanate and potassium tetrachloridoplatinate(II) were commercially available. Calf thymus DNA (CT-DNA), Tris-HCl and NaCl were purchased from Aldrich.

Synthesis of compounds

3,5-Diacetyl-1,2,4-triazol bis(^4N-tolylthiosemicarbazone) ligands. The thiosemicarbazides were prepared by reacting an ethanolic solution of the desired (*ortho*, *meta* or *para*) tolylisothiocyanate with an ethanolic solution of hydrazine hydrate, in a 1:1 molar ratio. The reaction mixture was stirred for one more hour and then the white product formed was filtered, washed with ethanol and diethyl ether, dried *in vacuo* and recrystallised from ethanol.

The thiosemicarbazones were obtained by refluxing an ethanolic solution (20 mL) of the desired ^4N-tolylthiosemicarbazide (2 mmol) with 3,5-diacetyl-1,2,4-triazol (1 mmol), which was prepared as described in reference,[25] for five hours and then was left to stand to ambient temperature. The solution was reduced to half volume and the pale yellow solid formed was filtered, washed with cold ethanol and diethyl ether and dried *in vacuo*.

3,5-diacetyl-1,2,4-triazol bis(^4N-*o*-tolylthiosemicarbazone), H$_5$L^1: yield (70%), mp 220 °C. Elemental analysis found, C, 54.95; H, 5.41; N, 23.75; S, 12.80; C$_{22}$H$_{25}$N$_9$S$_2$·EtOH requires C, 54.85; H, 5.95, N, 23.95; S 12.15%. MS (FAB$^+$ with *m*NBA matrix) *m/z* 480.2 (43%) for [C$_{22}$H$_{25}$N$_9$S$_2$+H]$^+$. IR (KBr pellet): ν/cm^{-1} 3521 (s, OH-EtOH), 3340 (s, NH-triazol), 3224 and 3172 (s, ^{2}NH and ^{4}NH), 1586 (s, CN), 857 (w, CS-thioamide IV band). ^{1}H NMR (300 MHz, DMSO-d_6): δ (ppm) 15.09 (s, NH-triazol, 1H), 12.92 and 11.35 (s, ^{2}NH, 1H), 10.23 and 10.09 (s, ^{4}NH, 1H), 7.27-7.20 (m, aromatic protons, 8H), 3.30 (s, CH$_3$-thiosemicarbazide, 6H), 2.23 and 2.22 (s, CH$_3$-triazol, 3H). UV–vis (DMSO): λ max/nm 295, 322.

3,5-Diacetyl-1,2,4-triazol bis(^4N-*m*-tolylthiosemicarbazone) H$_5$L^2: yield (60%), mp 194 °C. Elemental analysis found, C, 55.00; H, 5.50, N, 24.35; S 12.50; C$_{22}$H$_{25}$N$_9$S$_2$·EtOH requires C, 54.85; H, 5.95, N, 23.95; S 12.15%. MS (FAB$^+$ with *m*NBA matrix) *m/z* 480.1 (100%) for [C$_{22}$H$_{25}$N$_9$S$_2$+H]$^+$. IR (KBr pellet): ν/cm^{-1} 3584 (s, OH-EtOH), 3379 (s, NH-triazol), 3286 and 3197 (s, ^{2}NH and ^{4}NH), 1606 (s, CN), 756 (w, CS-thioamide IV band). ^{1}H NMR (300 MHz, DMSO-d_6): δ (ppm) 15.28 (s, NH-triazol, 1H), 12.91 and 11.27 (s, ^{2}NH, 1H), 10.30 and 10.19 (s, ^{4}NH, 1H), 7.47-7.00 (m, aromatic protons, 8H), 3.32 (s, CH$_3$-thiosemicarbazide, 6H), 2.43 and 2.31 (s, CH$_3$-triazol, 3H). UV–vis (DMSO): λ max/nm 323.

3,5-Diacetyl-1,2,4-triazol bis(^4N-*p*-tolylthiosemicarbazone) H$_5$L^3: yield (70%), mp 189 °C. Elemental analysis found, C, 55.00; H, 5.45, N, 24.10; S 12.50; C$_{22}$H$_{25}$N$_9$S$_2$·EtOH requires C, 54.85; H, 5.95, N, 23.95; S 12.15%. MS (FAB$^+$ with *m*NBA matrix) *m/z* 480.0 (35%) for [C$_{22}$H$_{25}$N$_9$S$_2$+H]$^+$. IR (KBr pellet): ν/cm^{-1} 3592 (s, OH-EtOH), 3360 (s, NH-triazol), 3237 and 3129 (w, ^{2}NH and ^{4}NH), 1588 (s, CN), 879 (w, CS-thioamide IV band). ^{1}H NMR (300 MHz, DMSO-d_6): δ (ppm) 15.27 (s, NH-triazol, 1H), 12.89 and 11.25 (s, ^{2}NH, 1H), 10.28 and 10.19 (s, ^{4}NH, 1H), 7.49–7.14 (m, aromatic protons, 8H), 3.22 (s, CH$_3$-thiosemicarbazide, 6H), 2.43 and 2.33 (s, CH$_3$-triazol, 3H). UV–vis (DMSO): λ max/nm 323.

Platinum(II) complexes. They were obtained by reacting a methanol (20 mL) suspension of the desired ligand with a water solution (5 mL) of potassium tetrachloridoplatinate(II). The reaction mixture was stirred at room temperature in the dark for 5 h. The resulting orange solid obtained was filtered, washed with methanol and diethyl ether and dried *in vacuo*. Finally it was crystallized by slow evaporation from a DMSO solution.

[Pt(μ-H$_3$L^1)]$_2$: yield (45%), mp 300 °C (decomposes). Elemental analysis found, C, 39.65; H, 4.00, N, 19.25; S 9.55; C$_{44}$H$_{50}$N$_{18}$S$_4$Pt$_2$ requires C, 39.15; H, 3.75; N, 18.65; S 9.50%. Molar conductivity (DMF: 10^{-3} M, μS cm^{-1}): 13. IR (KBr pellet): ν/cm^{-1} 3176 (w, NH), 1585 (s, CN). ^{1}H NMR (300 MHz, DMSO-d_6): δ (ppm)

15.11 (s, NH-triazol, 0.5H), 12.92 (s, ^{2}NH, 0.5H), 11.34 (s, ^{2}NH, 1H), 10.23 and 10.09 (s, ^{4}NH, 2H), 7.27–7.21 (m, aromatic protons, 16H), 3.60 (s, CH$_3$-thiosemicarbazide, 12H), 2.41 (s, CH$_3$-triazol, 12H). UV–vis (DMSO): λ max/nm 323.

[Pt(μ-H$_3$L^2)]$_2$: yield (55%), mp 259 °C (decomposes). Elemental analysis found, C, 38.90; H, 3.85, N, 19.25; S 9.50; C$_{44}$H$_{50}$N$_{18}$S$_4$Pt$_2$ requires C, 39.15; H, 3.75, N, 18.65; S 9.50%. Molar conductivity (DMF: 10^{-3} M, μS cm^{-1}): 21. IR (KBr pellet): ν/cm^{-1} 3197 (w, NH), 1607 (s, CN). ^{1}H NMR (300 MHz, DMSO-d_6): δ (ppm) 15.30 (s, NH-triazol, 0.5H), 12.91 (s, ^{2}NH, 0.5H), 11.27 (s, ^{2}NH, 1H), 10.30 and 10.20 (s, ^{4}NH, 2H), 7.47–7.00 (m, aromatic protons, 16H), 3.45 (s, CH$_3$-thiosemicarbazide, 12H), 2.35 and 2.31 (s, CH$_3$-triazol, 12H). UV–vis (DMSO, λ max/nm) 320.

[Pt(μ-H$_3$L^3)]$_2$: yield (55%), mp 292 °C (decomposes). Elemental analysis found, C, 38.50; H, 4.55, N, 16.50; S 12.70; C$_{44}$H$_{50}$N$_{18}$S$_4$Pt$_2$·2DMSO requires C, 38.30; H, 4.15, N, 16.75; S 12.75%. Molar conductivity (DMF: 10^{-3} M, μS cm^{-1}): 09. IR (KBr pellet): ν/cm^{-1} 3234 (w, NH), 1592 (s, CN). ^{1}H NMR (300 MHz, DMSO-d_6): δ (ppm) 15.30 (s, NH-triazol, 0.5H), 12.90 (s, ^{2}NH, 0.5H), 11.25 (s, ^{2}NH, 1H), 10.30 and 10.19 (s, ^{4}NH, 2H), 7.49–7.15 (m, aromatic protons, 16H), 3.48 (s, CH$_3$-thiosemicarbazide, 12H), 2.33 and 2.30 (s, CH$_3$-triazol, 12H). UV–vis (DMSO, λ max/nm) 322.

Crystallography

A summary of the crystal data collection and refinement parameters for complex [Pt(μ-H$_3$L^3)]$_2$ is given in Table 1. The crystals were placed in a Bruker–Nonius X8 APEX II CCD area-detector diffractometer equipped with a graphite-monochromated Mo-Kα radiation source (λ = 0.71073 Å). Data were integrated using SAINT[26] which also applied corrections for Lorentz and polarization effects. An absorption correction was performed with the program SADABS.[27] The software package SHELXTL[28] was used for space group determination, structure solution, and refinement. The structure was solved by direct methods, completed with different Fourier syntheses, and refined with anisotropic displacement parameters. The position of the hydrogen atoms were calculated geometrically and were allowed to ride on their parent carbon atoms with fixed isotropic U.

Refinement included application of the squeeze procedure[29] to model diffuse electron density in one substantial void per unit cell presumably occupied by disordered DMSO solvent molecules. Chemical formula and derivate quantities are given without solvent.

CCDC-805583 contains the supplementary crystallographic data for **[Pt(μ-H$_3$L^3)]$_2$** compound described in this paper (please see ESI†). These data can be obtained free of charge at www.ccdc.cam.ac.uk/conts/retrieving.html [or from the Cambridge Crystallographic Data Centre, 12, Union Road, Cambridge CB2 1EZ, UK; fax: +44-1223/336-033; E-mail: deposit@ccdc.cam.ac.uk].

In vitro antiproliferative activity

The human cancer cells (A2780, A2780cisR and NCI-H460) were grown in RPMI-1640 medium supplemented with 10% foetal bovine serum (FBS) and 2 mM L-glutamine in an atmosphere of 5% CO$_2$ at 37 °C. Cell proliferation was evaluated by the sulforhodamine B assay. Cells were plated in 96-well sterile plates at a density of 15×10^3 (for NCI-H460) or 4000 (for A2780 and A2780cisR) cells per well with 100 μL of medium and were then incubated for 24 h. After attachment to the culture surface the cells were incubated with various concentrations of the compounds tested freshly dissolved in DMSO (1 mg mL^{-1}) and diluted in the culture medium (DMSO final concentration 1%) for 48 h (for NCI-H460) or 96 h (for A2780 and A2780cisR). The cells were fixed by adding 50 μL of 30% trichloroacetic acid (TCA) per well. The plates were incubated at 4 °C for 1 h and then washed five times with distilled water. The cellular material fixed with TCA was stained with 0.4% sulforhodamine B dissolved in 1% acetic acid for 10 min. Unbound dye was removed by rinsing with 0.1% acetic acid. The protein-bound dye was extracted with 10 mM unbuffered Tris base for determination of optical density (at 515 nm) in a Tecan Ultra Evolution spectrophotometer.

The normal human cells (LLC-PK1) were grown in 199 medium supplemented with 3% foetal bovine serum (FBS) and 1.5 g L^{-1} of sodium bicarbonate in an atmosphere of 5% CO$_2$ at 37 °C. Cell proliferation was evaluated by the sulforhodamine B assay. Cells were plated in 96-well sterile plates at a density of 10,000 cells per well with 100 μL of medium and were then incubated for 24 h. After attachment to the culture surface the cells were incubated with various concentrations of the compounds tested freshly dissolved in DMSO (1 mg mL^{-1}) and diluted in the culture medium (DMSO final concentration 1%) for 48 h at 37 °C. The cells were fixed by adding 50 μL of 30% trichloroacetic acid (TCA) per well. The plates were incubated at 4 °C for 1 h and then washed five times with distilled water. The cellular material fixed with TCA was stained with 0.4% sulforhodamine B dissolved in 1% acetic acid for 10 min. Unbound dye was removed by rinsing with 0.1% acetic acid. The protein-bound dye was extracted with 10 mM unbuffered Tris base for determination of optical density (at 515 nm) in a Tecan Ultra Evolution spectrophotometer.

The effects of complexes were expressed as corrected percentage inhibition values according to the following equation:

$$\% \text{ Inhibition} = [1 - (T/C)] \times 100$$

where T is the mean absorbance of the treated cells and C the mean absorbance in the controls.

The inhibitory potential of compounds was measured by calculating concentration–percentage inhibition curves, these curves were adjusted to the following equation:

$$E = E\text{max}/[1 + (IC_{50}/C)^n]$$

where E is the percentage inhibition observed, $E_{\max}$ is the maximal effects, IC_{50} is the concentration that inhibits 50% of maximal growth, C is the concentration of compounds tested and n is the slope of the semi-logarithmic dose–response sigmoid curves. This non-linear fitting was performed using GraphPad Prism 2.01 software.[30]

For comparison purposes, the antiproliferative activity of cisplatin was evaluated under the same experimental conditions. All compounds were tested in two independent studies with triplicate points. These experiments were carried out at the Unidad de Evaluación de Actividades Farmacológicas de Compuestos Químicos (USEF), Universidad de Santiago de Compostela.

DNA-Binding experiments

CT-DNA stock solution was prepared by dissolving the lyophilized sodium salt in Tris-buffer (NaCl 50 mM, Tris-HCl 5 mM, pH was adjusted to 7.3 with NaOH 0.5 M) by stirring at 4 °C for 2 days. The CT-DNA solution was standardized spectrophotometrically[31] by using its known molar absorption coefficient at 260 nm (6600 M^{-1} cm^{-1}). The ratio of UV absorbance at 260 and 280 nm, A_{260}/A_{280}, of ca. 1.8, indicating that the DNA was sufficiently free of protein. Stock solutions were kept frozen until the day of the experiment.

Concentrated stock solutions (5×10^{-3} M) of both ligands and platinum(II) complexes were prepared dissolving each one of the compounds in DMSO. From these stock solutions, for all experiments the desired concentration of compound was achieved by dilution with Tris-buffer (NaCl 50 mM, Tris-HCl 5 mM, pH was adjusted to 7.3 with NaOH 0.5 M) to give homogeneous solutions with a DMSO content of less than 2.5%.

In order to prepare the adducts with double-stranded CT-DNA, to a mixture of a fixed amount of CT-DNA (1×10^{-4} M) in Tris buffer were added predetermined quantities of the desired compound solution to achieve different R values (R = [CT-DNA]/[compound]). The mixtures were incubated for 10 min at 37 °C, and the their UV-vis absorption spectra were recorded, at room temperature, in the wavelength interval of 240–400 nm.

Acknowledgements

References

1 N. J. Wheate, S. Walker, G. E. Craig and R. Oun, *Dalton Trans.*, 2010, **39**, 8113–8127.
2 E. Wong and C. M. Giandomenico, *Chem. Rev.*, 1999, **99**, 2451–2466.
3 Z. Guo and P. J. Sadler, *Angew. Chem., Int. Ed.*, 1999, **38**, 1512–1531.
4 M. S. Razzaque, *Nephrol. Dial. Transplant.*, 2007, 1–5.
5 M. Okuda, K. Masaki, S. Fukatsu, Y. Hashimoto and K. Inui, *Biochem. Pharmacol.*, 2000, **59**, 195–201.
6 K. von der Schilden, F. García, H. Kooijman, A. L. Spek, J. G. Haasnoot and J. Reedijk, *Angew. Chem., Int. Ed.*, 2004, **43**, 5668–5670.
7 J. M. Pérez, V. Cerrillo, A. I. Matesanz, J. M. Millán, P. Navarro, C. Alonso and P. Souza, *ChemBioChem*, 2001, **2**, 119–123.
8 T. W. Hambley, *Coord. Chem. Rev.*, 1997, **166**, 181–223.
9 J. Kasparkova, V. Marini, Y. Najajreh, D. Gibson and V. Brabec, *Biochemistry*, 2003, **42**, 6321–6332.
10 C. Marzano, A. Trevisan, L. Giovagnini and D. Fregona, *Toxicol. in Vitro*, 2002, **16**, 413–419.
11 J. S. Casas, E. E. Castellano, J. Ellena, M. S. García-Tasende, M. L. Pérez-Parallé, A. Sánchez, A. Sánchez-González, J. Sordo and A. Touceda, *J. Inorg. Biochem.*, 2008, **102**, 33–45.
12 M. Liu, T. Lin and A. C. Sartorelli, *Prog. Med. Chem.*, 1995, **32**, 1–35.
13 R. A. Finch, M. C. Liu, A. H. Cory, J. G. Cory and A. C. Sartorelli, *Adv. Enzyme Regul.*, 1999, **39**, 3–12.
14 R. A. Finch, M. C. Liu, S. P. Grill, W. C. Rose, R. Loomis, K. M. Vasquez, Y. C. Cheng and A. C. Sartorelli, *Biochem. Pharmacol.*, 2000, **59**, 983–991.
15 A. B. Alvero, W. Chen, A. C. Sartorelli, P. Schwartz, T. Rutherford and G. Mor, *J. Soc. Gynecol. Invest.*, 2006, **13**, 145–152.
16 A. I. Matesanz and P. Souza, *Mini-Rev. Med. Chem.*, 2009, **9**, 1389–89.
17 A. I. Matesanz and P. Souza, *J. Inorg. Biochem.*, 2007, **101**, 245–253.
18 B. Singh, M. M. P. Rukhaiyar and R. J. Sinhal, *J. Inorg. Nucl. Chem.*, 1977, **39**, 29–32.
19 R. P. Tenorio, A. J. S. Goes, J. G. de Lima, A. R. de Faria, A. J. Alves and T. M. Aquino, *Quim. Nova*, 2005, **28**(6), 1030–1037.
20 L. Papathanasis, M. A. Demertzis, P. N. Yadav, D. Kovala-Demertzi, Ch. Prentjas, A. Castiñeiras, S. Skoulika and D. X. West, *Inorg. Chim. Acta*, 2004, **357**, 4113–4120.
21 D. Kovala-Demertzi, M. A. Demertzis, J. R. Miller, C. Papadopoulou, C. Dodorou and G. Filousis, *J. Inorg. Biochem.*, 2001, **86**, 555–563.
22 A. I. Matesanz, C. Joie and P. Souza, *Dalton Trans.*, 2010, **39**, 7059–7065.
23 A. I. Matesanz, J. Mosa, I. García, C. Pastor and P. Souza, *Inorg. Chem. Commun.*, 2004, **7**, 756–759.
24 F. Arjmand and M. Aziz, *Eur. J. Med. Chem.*, 2009, **44**, 834–844.
25 J. M. Alonso, M. R. Martin, J. de Mendoza, T. Torres and J. Elguero, *Heterocycles*, 1987, **26**, 989–1000.
26 SAINT+ v7.12a. *Area-Detector Integration Program*. Bruker-Nonius AXS. Madison, Wisconsin, USA, 2004.
27 G. M. Sheldrick, SADABS version 2004/1. *A Program for Empirical Absorption Correction*. University of Göttingen, Göttingen, Germany, 2004.
28 SHELXTL-NT version 6.12. *Structure Determination Package*. Bruker-Nonius AXS. Madison, Wisconsin, USA, 2001.
29 A. L. Spek, *J. Appl. Crystallogr.*, 2003, **36**, 7–13.
30 *GraphPad Prism*, version 2.01. 1996. GraphPad Software, Inc., San Diego, CA.
31 M. E. Reichmann, S. A. Rice, C. A. Thomas and P. Doty, *J. Am. Chem. Soc.*, 1954, **76**, 3047.